Effects of solvent on the conformation and the collective motions of a protein. 2. Structure of hydration in melittin

ARTICLE *in* THE JOURNAL OF PHYSICAL CHEMISTRY · SEPTEMBER 1993

Impact Factor: 2.78 · DOI: 10.1021/j100141a052

3 AUTHORS, INCLUDING:

Akio Kitao
The University of Tokyo
95 PUBLICATIONS **2,557** CITATIONS
SEE PROFILE

Nobuhiro Go
Japan Atomic Energy Agency
238 PUBLICATIONS **9,961** CITATIONS
SEE PROFILE

Effects of Solvent on the Conformation and the Collective Motions of a Protein. 2. Structure of Hydration in Melittin

Akio Kitao, Fumio Hirata, and Nobuhiro Gō*

Department of Chemistry, Faculty of Science, Kyoto University, Sakyo-ku, Kyoto 606-01, Japan

Received: April 8, 1993•

The dynamic correlation of solvent molecules with the collective motions of a protein is studied on the basis of a molecular dynamics simulation. Our attention is focused especially on the response of the solvent molecules to the conformational transition of the protein, which has been observed in a 50-psec trajectory projected onto low-frequency collective modes (*Chem. Phys.* **1991**, *158*, 447). It is shown that the conformational transition is associated with an extensive change in the atom packing and the hydrogen-bond network between protein and water molecules.

I. Introduction

There is growing interest in the influence that a solvent environment exerts on the structure and dynamics of a protein. Fluctuations with various different time scales taking place in biomolecules are expected to be closely correlated with solvent dynamics. Computer experiments, such as the method of molecular dynamics, are the most powerful tools for exploring such correlations at the molecular level.[1,2]

In the preceding paper,[3] we have reported a molecular dynamics (MD) study of melittin in water. Melittin is a bioactive polypeptide consisting of 26 amino acid residues with the sequence NH_3-Gly-Ile-Gly-Ala-Val-Leu-Lys-Val-Leu-Thr-Thr-Gly-Leu-Pro-Ala-Leu-Ile-Ser-Trp-Ile-Lys-Arg-Lys-Arg-Gln-Gln-NH_2 and is a main component of bee venom. Analysis of the result was focused mainly on the effect of solvent on the collective motion of the solute. The MD trajectory of the protein was projected onto the axes of a few lowest frequency modes, which were defined either by principal component analysis or by normal-mode analysis. The analysis revealed some interesting characteristics of the collective motion of the protein in water. The projected trajectory of the dynamics in water showed a diffusive character, associated with a clear transition from one conformation to another. The result strongly suggests changes of the potential surface of the protein due to the solute–solvent interaction. It was also observed that the time correlation functions for the collective motions are overdamped. These two results indicate that time evolution of protein motion in water is significantly different from that in vacuum.

It is of great interest to see how the collective motion of the solute is correlated with the dynamics of solvent molecules. As for small molecules in water, numerous studies have already been devoted to elucidate the structure and dynamics of a solvent around solute molecules, including inert gas,[4] small ions,[5] and alanine dipeptide.[6] However, these studies are concerned mainly with local structures and dynamics of the solvent around a solute atom. In this article, we attempt to characterize the dynamic response of solvent molecules to the structural fluctuations of a protein in low-frequency modes.

In the MD simulation of water, we obtain a series of snapshots, which are called instantaneous structures (I-structures).[7] Both rapid vibrational (librational and rotational) motions and relatively slow motions involving the change of the hydrogen-bond network are taking place in the time series of I-structure. At room temperature, the time scale of the rapid librational and rotational motions of water molecules are well separated from that of slow and large motions taking place in the range of picoseconds or longer. The present study concerns the correlation of the water dynamics to the collective motions of the protein that are taking place in time range of picosecond or longer. It is therefore advantageous to separate the slow motions of water molecules from the rapid vibrational motions, which are expected to be less important in coupling with the collective motions of the protein. Such separation can be carried out by averaging the trajectory (I-structure) over a time period characteristic to the vibrational motions. The averaged structures are called vibrationally averaged structures (V-structures).[7,8] In the present study, we carry out the vibrational average for protein and ions as well as for water molecules.

Melittin consists of two α-helical regions connected by Thr11 and Gly12. Melittin is an amphipathic molecule. Hydrophilic residues exist mainly in the outer side of the bend, and hydrophobic residues exist mainly in the inner side. We call the outer side and inner side "hydrophilic side" and "hydrophobic side", respectively. The collective motions of melittin are bending motions causing changes of angles formed by the two α-helical regions.[3,9]

II. Methods

A. Simulation. We have carried out two MD simulations: the MD of pure water and that of water and melittin.[3] Both simulations are carried out by using the program IMPACT.[10] In the MD of pure water, 216 simple point charge[11] (SPC) water molecules are simulated with periodic boundary conditions in a box of 18.6 Å × 18.6 Å × 18.6 Å. In another MD, one melittin molecule, six chloride ions, and 1304 water molecules are simulated with periodic boundary conditions in a box of 29.0 Å × 30.1 Å × 50.7 Å. Six chloride ions are initially placed at positions where they are in contact with six positively charged groups, $-NH_3^+$ groups of N-terminus and three Lys's and NH_2 groups of two Arg's. In both simulations, the numerical integration of the Newton equation is carried out by taking time steps of 1 fs. The shape of water molecules is kept rigid by the RATTLE[12] algorithm. The system is weakly coupled to a heat bath in order to keep the temperature constant at 300 K by Berendsen's method[13] with a relaxation time 0.01 ps. The Lennard-Jones and electrostatic energies are smoothly cut off[10] at 9 Å. The list of nonbonded interactions is updated at every 5 steps. The relative dielectric constant is 1.0. After 84-ps equilibration, the N-terminus, Lys7, and Lys21 are each in contact with one chloride ion and Arg22 is in contact with two chloride ions. Lys23 and Arg24 are out of contact with chloride ions. One chloride ion is located at the position between the charged groups of Lys23 and Arg24. After equilibration, the trajectory data of

* Author to whom correspondence should be addressed.
• Abstract published in *Advance ACS Abstracts*, September 1, 1993.

0022-3654/93/2097-10223$04.00/0

I-structures are collected over 50 psec and are employed for the following analyses.

B. V-Structure. Coordinates of the V-structure are calculated by taking the averages of dynamical variables as follows:[14]

$$\bar{q}_i(t) = \int_{-\Delta\tau}^{\Delta\tau} \frac{\sin(\pi t'/\Delta\tau)}{\pi t'/\Delta\tau} q_i(t+t')\,dt' \Big/ \int_{-\Delta\tau}^{\Delta\tau} \frac{\sin(\pi t'/\Delta\tau)}{\pi t'/\Delta\tau}\,dt' \quad (1)$$

where $q_i(t)$ is one of the dynamical variables describing I-structures. In this calculation, $\Delta\tau$ is taken to be 0.2 ps. Before the averaging is done, external, i.e., translational, rotational, and internal motions of each molecule are separated. Because the model of the water molecule in this paper is rigid, it has no internal motion. The translational and rotational motions of a water molecule are given by the Cartesian coordinates of the center of mass and the quarternions.[15] To define external motions of the protein, we first define its reference conformation as the average conformation over a 50-ps simulation. Transitional and rotational motions are defined as Cartesian coordinates of the center of mass and the quarternions of the reference conformation when the latter is brought into the mass-weighted best-fit spatial position and orientation with each of the I-structures (the Eckart condition[16]). Internal motion is expressed by Cartesian coordinates of each atom with respect to the coordinate system fixed to the reference conformation in its best-fit position with the I-structure. After the separation, the averaging is done for both external and internal variables by eq 1. Distortions of bond lengths and bond angles from the standard values, which may occur as a result of averaging, are found to be negligibly small. We constructed 922 V-structures every 50 fs from the record of the 50-ps MD trajectory to be used in the following analyses.

C. Atom Packing and Hydrogen-Bond Network. We define contact of atoms or atom packing as follows. The Lennard-Jones 12–6 energy parameters are defined by

$$E_{ij} = 4\epsilon_{ij}\left\{\left(\frac{\sigma_{ij}}{r_{ij}}\right)^{12} - \left(\frac{\sigma_{ij}}{r_{ij}}\right)^{6}\right\} \quad (2)$$

where E_{ij} is the Lennard-Jones energy, ϵ_{ij} is the depth of the potential minimum, and σ_{ij} is the contact distance parameter of an atom pair i and j. The last is obtained from the diameter of the two atoms based on the Lorentz–Berthelot rule $\sigma_{ij} = (\sigma_i + \sigma_j)/2$. When the distance r_{ij}, between atom i and atom j, not connected directly by a chemical bond, satisfies the condition

$$r_{ij} \le k\sigma_{ij} \quad (3)$$

the two atoms are defined to be in contact or to be in atom packing positions, where k is a constant determined from the radial distribution functions. We do not pay attention to atom packing of water hydrogen atoms, because the Lennard-Jones diameter of a hydrogen atom of SPC water is zero. In the definition of atom packing between protein and water atoms (protein–water packing) or between water molecules (water–water packing), judging from the radial distribution functions obtained in this calculation, we select a value of 1.2 for the factor k. In the case of water–water packing, the criterion of the O–O distance, $k\sigma_{ij}$, is 3.8 Å. At this distance, pair energy is about half the minimum pair energy. In the case of ion–water or ion–protein pairs, we find that $k = 1.1$ is an appropriate value, which we also determine from the radial distribution functions. The change of the intramolecular packing topology of the protein has been reported to be important in the conformational changes of bovine pancreatic trypsin inhibitor, a globular protein consisting of 58 amino acid residues.[17] As we mentioned in the previous paper,[3] we checked the change of intramolecular packing topology in melittin, but no appreciable changes were observed. For this reason we consider here only the changes of the intermolecular packing topology.

We define a hydrogen bond to exist between a pair of water molecules (water–water H-bond), if two water oxygen atoms are in contact (distance criterion) and the pair energy is less than −3.0 kcal/mol (energy criterion). The pair energy is a sum of Lennard-Jones 12–6 interaction energies and Coulomb interaction energies over all pairs of atoms between the two molecules. A water molecule is regarded as hydrogen bonded (protein–water H-bond) to melittin when the water molecule and one polar or charged group of melittin listed in Table I are in contact with at least one pair of atoms and the pair energy between the water and the group is less than −3.0 kcal/mol. The definition of pair energy is the same as in the case of a water–water H-bond. A combination of the distance and angle only, with no energy criterion, has often been employed in the case of protein–water hydrogen-bond analysis of I-structures.[2] Among the many types of hydrogen-bonding pairs occurring in our problem, there are cases where the intergroup energy is appreciably high even when both distance and angle criteria are satisfied. We found that these cases can be eliminated by employing the distance and the energy criteria.

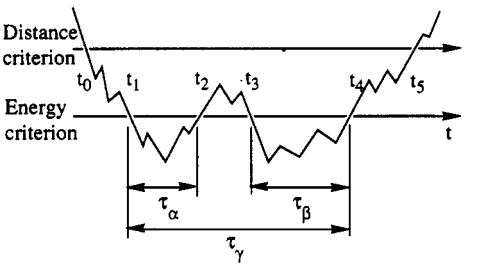

Figure 1. Schematic drawing of the hydrogen-bond definition. Lifetimes of the hydrogen bond in definition I are τ_α, τ_β and that of definition II is τ_γ. See the text for details.

TABLE I: List of Charged and Polar Groups

	residue	group
charged groups		
main chain	N-terminus	$-NH_3^+$
side chain	Lys	$-NH_3^+$
	Arg	$-NHC(NH_2)=NH_2^+$
polar groups		
main chain	all except for Pro	>NH
	all	>CO
	C-terminus	$-NH_2$
side chain	Thr	−OH
	Ser	−OH
	Gln	−CO
		−NH

The lifetimes of H-bonds are calculated by two different definitions. Definition I: Count lifetime I only when both distance and energy criteria are satisfied (for example, τ_α from t_1 to t_2 and τ_β from t_3 to t_4 in Figure 1). Definition II: At first, identify the duration of time whereby the distance criterion is continuously satisfied (from t_0 to t_5). Then identify the time t_1, when both the distance and energy criteria first become satisfied after t_0, and the time t_4, when the energy criterion is violated for the final time before t_5. Lifetime II is defined as the duration between t_1 and t_4. Lifetime II may be longer than that in definition I, because the former covers a duration where the pair energy may be higher than the energy criterion.

D. Classification of Water Molecules. The protein molecule contains several types of atom groups that interact in different ways with the water molecules. Therefore it is important to classify water molecules into several classes according to the atom groups with which the solvent molecules are interacting. Such a classification was done also for water molecules around a dipeptide by Rossky and Karplus.[6] We classify water molecules around protein in each V-structure into seven classes. The

TABLE II: Average Number of Water Molecules in Each Class

class	av no. of molecules	fractn, %
C1 (charged1)	64.7 ± 3.1	5.0
P1 (polar 1)	34.6 ± 3.3	2.7
N1 (nonpolar1)	77.4 ± 6.1	5.9
C2 (charged2)	84.3 ± 5.1	6.5
P2 (polar2)	42.1 ± 4.7	3.2
N2 (nonpolar2)	92.4 ± 7.2	7.2
bulk	908.5 ± 11.0	69.5
pure	216	

following seven classes are rank-ordered in the order of the following definitions in the sense that a molecule that can be classified into two or more classes is classified into the earliest class. A water molecule that is in contact with either a chloride ion or a charged group is called C1 (charged1) water. A water molecule in contact with a polar group is called P1 (polar1) and that with a nonpolar group is called a N1 (nonpolar1) water molecule. These three classes of water molecules are the first-shell water molecules. A water molecule in contact with a C1 water molecule is called C2 (charged2), that with P1 water molecule P2 (polar2), and that with N1 water molecule N2 (nonpolar2). These three kinds of water molecules are called the second-shell water molecules. The rest of the water molecules are called bulk water molecules. Water molecules simulated in the MD of pure water are called pure water molecules.

III. Results and Discussion

A. Water Molecules in Each Class. The average number of water molecules that belong to each class is shown in Table II. C1, P1, and N1 water molecules are also shown in Figure 2. The N-terminus of melittin is located to the left of the figure. C1 water molecules form two groups as seen in Figure 2a. One group is located near the N-terminus and Lys7. Another is located near Lys21, Arg22, Lys23, and Arg24. P1 water molecules are all located on the "hydrophilic side". They form mainly three groups. The first group is located near the N-terminus. The water molecules in this group are in contact with H^N's of Gly1, Ile2, Gly3, and Ala4. The H^N atoms of the first four residues have no partner to form intra-α-helical H-bonds. The second group can be seen at the junction of the two α-helices. The water molecules in this group are in contact with polar groups in the side chains of Thr10, Thr11, Ser18, and main chain CO of Leu9, Thr10, and Thr11. The third group is located near the C-terminus. N1 water molecules are those that do not belong to either charged or polar groups among water molecules in the first shell type.

B. Average Hydration Structure. To obtain some insight about hydration structures, we calculate radial distribution functions for various types of atoms. It has been reported that the width and the height of the peaks in radial distribution functions obtained for V-structures of pure liquid water are narrower and higher than those of I-structures.[8] This has been interpreted to mean that suppression of the high-frequency translational and librational motions of water molecules reveals the structure intrinsic to the liquid water. Therefore, we also calculate radial distribution functions for both V-structures and I-structures. Examples of the radial distribution functions between a protein atom and oxygen atoms of water molecules are shown in Figure 3. In Figure 3, the radial distribution functions of the oxygen atom of water molecules around the N^η atom in Arg residues (a), around the C^δ atom in Leu residues (b), and around the C^β atom in Ala residues (c) are shown. The radial distribution functions around other charged or polar atoms in melittin are similar to (a). The first peak for the V-structures is found to be narrower and higher than that for the I-structures as in the case of pure water. The radial distribution functions around methyl groups in Val and Ile

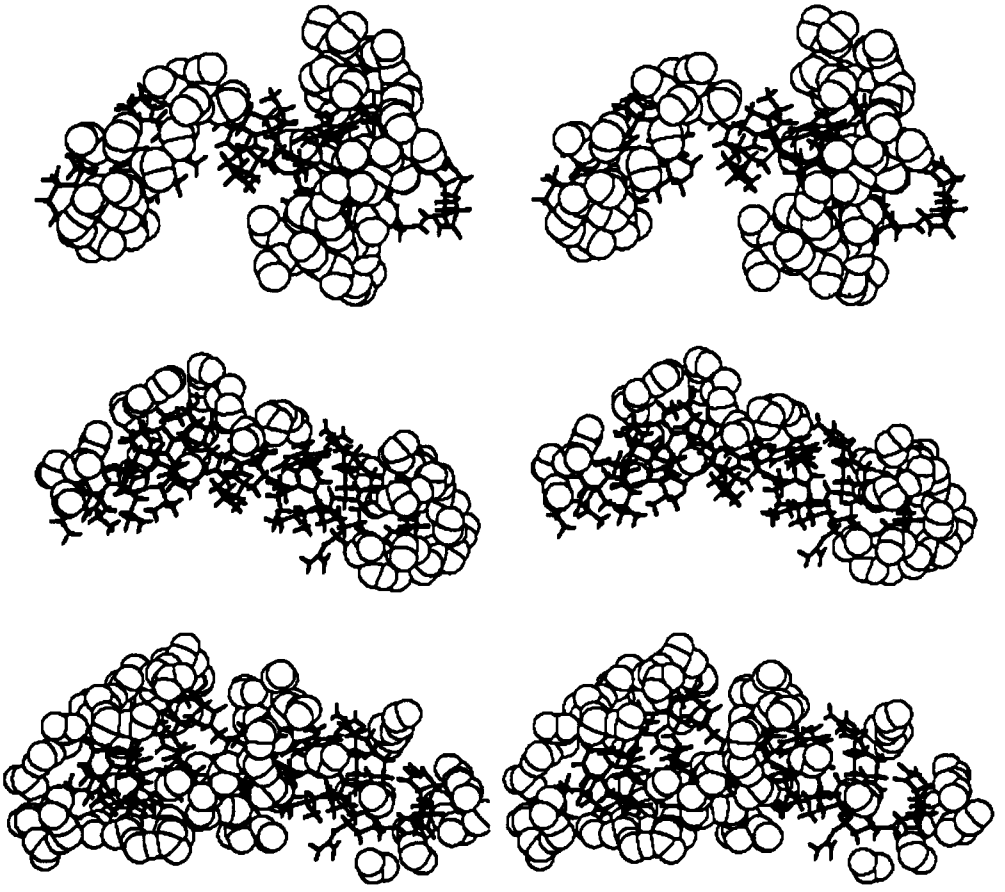

Figure 2. Stereoview of (a, top) C1 (charged1), (b, middle) P1 (polar1), and (c, bottom) N1 (nonpolar1) water molecules shown in the CPK model. Melittin is shown by the wire model. This conformation is a V-structure averaged from 0.0 to 0.4 ps in simulation time.

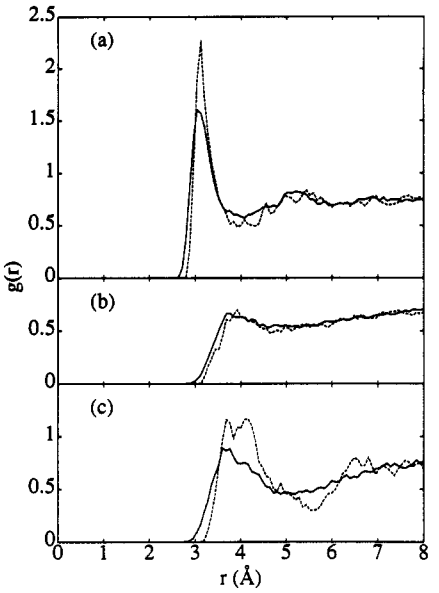

Figure 3. Radial distribution functions of O of water molecules around (a) N^{η} in Arg residues, (b) C^{δ} in Leu residues, and (c) C^{β} in Ala residues. The lines (—) show the results in the I-structure and the lines (- - -) show the results in the V-structure.

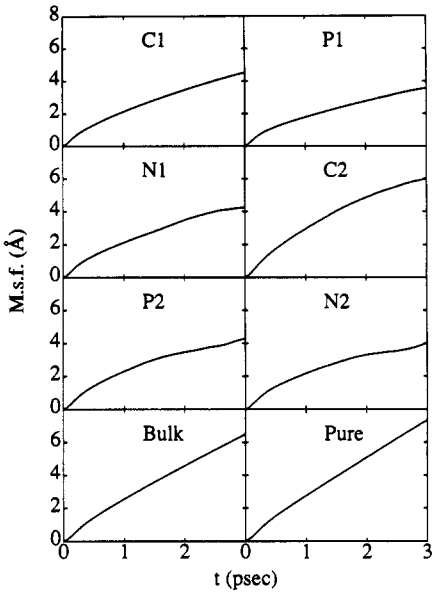

Figure 4. Mean-square fluctuation of center of mass of water molecules in each class.

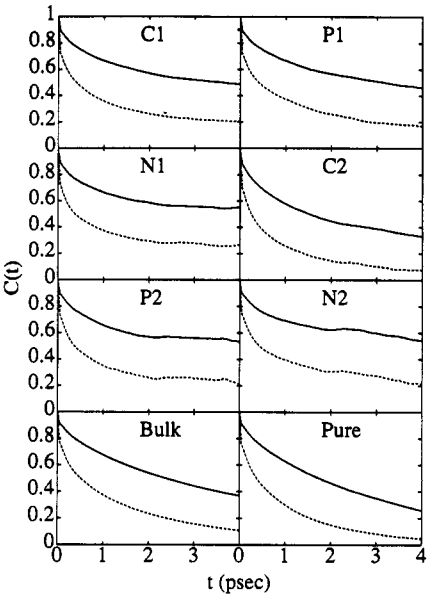

Figure 5. Time correlation functions of rotational motions. The lines (—) show $C_1(t)$ and the lines (- - -) show $C_2(t)$.

residues are similar to that in (b). The number of water molecules in the first shell, i.e., within r = 3.9 Å in (a) and within r = 4.6 Å in (b), are 4.5 and 4.7, respectively. The average accessible surface area (ASA) of four N^{η} atoms and eight C^{δ} atoms is found to be 43 and 36 Å^2, respectively. Therefore the number of water molecules per ASA in (a) is only slightly less than that in (b) but not significantly. However, the first sharp peak observed in (a) near r = 3.0 Å, which is not so sharp as in (b), indicates that water molecules around charged groups are located mainly at the position of the peak. The radial distribution function in (c) has a character between that in (a) and (b). This is because the Ala side chain (methyl group) is small. Water molecules around the methyl group can also be hydrogen-bonded to charged or polar groups. Some of the water molecules in contact with the methyl group of Ala4 or Ala15 are also in contact with the NH_3 group of Lys7 or both main-chain NH group and CO groups, respectively.

C. Translational and Rotational Motions of Water Molecules. In this section we examine the characteristics of the translational and rotational motions of water molecules in each class. The values shown in this section are calculated from the I-structures after classification of water molecules has been done for the corresponding V-structures. To examine the translational motions, we calculate the mean-square fluctuation (msf) of the center of mass positions. The obtained msf is averaged over water molecules belonging to the same class and the results are shown in Figure 4. The mean-square fluctuation of coordinates is related to the self-diffusion constant D, as $\langle(\mathbf{x}(t)-\mathbf{x}(0))^2\rangle = 6Dt + a$ $(t\rightarrow\infty)$, where $\mathbf{x}(t)$ is the position vector of center of mass coordinates and a is a certain constant. The curve of the msf from 1.0 to 3.0 ps is fitted to a straight line to give the diffusion constant. The obtained diffusion constant is shown in Table III.

The time correlation function for rotational motions, $C_l(t)$, is given as $C_l(t) = \langle P_l(\mathbf{u}(t)\cdot\mathbf{u}(0))\rangle = \langle P_l(\cos(\theta))\rangle$, where P_l is the Legendre polynomial of order l, $\mathbf{u}(t)$ is a unit vector of the dipole axis of a water molecule, and θ is the angle between $\mathbf{u}(t)$ and $\mathbf{u}(0)$, $C_1(t)$ and $C_2(t)$ are given by $\langle\cos\theta\rangle$ and $\langle(3\cos^2\theta - 1)/2\rangle$, respectively. These time correlation functions are calculated for each water molecule and then averaged over those belonging to each class. The obtained results are shown in Figure 5. The relaxation times are calculated by fitting the obtained time correlation functions to a single exponential function in the range from 1.0 to 3.0 ps. The obtained relaxation times, τ_1 and τ_2 (for $C_1(t)$ and $C_2(t)$, respectively), are shown also in Table III.

TABLE III: Characteristics of the Translational and Rotational Motions of Water Molecules

class	D, 10^{-5} cm^2/s	τ_1, psec	τ_2, psec
C1 (charged1)	2.7	4.1	1.7
P1 (polar1)	2.1	4.0	1.7
N1 (nonpolar1)	2.6	4.4	2.0
C2 (charged2)	3.7	2.8	1.2
P2 (polar2)	2.6	4.4	1.9
N2 (nonpolar2)	2.4	5.2	2.0
bulk	3.7	3.5	1.5
pure	4.0	3.0	1.4

In general, the translational motions of water molecules around the protein are slower than that of bulk water. The results are generally in accordance with those reported previously for BPTI[1b] and lysozyme.[1c] Further comparison is difficult because of the difference in the classification of water molecules. The diffusion constants of water molecules of the first shell and of P2 and N2 water molecules are smaller by about 40–50% than that of the bulk and pure water molecules. The relaxation times τ_1 and τ_2 of water molecules in the first and second shell are 1.2–1.7 times that of pure water, except for that of C2 water molecules. By

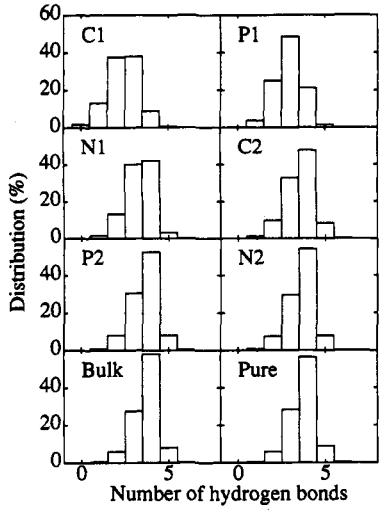

Figure 6. Histograms of the number of water–water hydrogen bonds for each class of water. Percentage of water molecules with a given value of hydrogen bonds is shown.

the ^{17}O NMR experiments of an aqueous solution of apolar amino acids and Gly peptides, a quantity comparable to τ_2 has been measured. The ratios of the measured τ_c against that of pure water are 1.14–1.87.[18] Thus, the values obtained in this simulation agree well with this experimental result. The diffusion constant of C2 water molecules is only slightly less than that of the pure water but not significantly. The relaxation times τ_1 and τ_2 of C2 water molecules are ~0.9 times those of pure water. These data indicate that C2 water molecules are less structured than other water molecules in the first and the second shells and also than bulk water molecules. This phenomenon may be attributed to so-called "structure breaking" [19] or "negative hydration effects".[20] The C1 and C2 water molecules interact with and are oriented to charged groups and chloride ions. Water–water structures are destroyed by this effect. The C1 water molecules are immobilized by the strong interaction with a charged group and/or a chloride ion. The C2 water molecules are not immobilized and their mobilities are increased by the destruction of the structure. The C1 and C2 regions are the so-called region of immobilization and the region of structure breaking, respectively.[19] The existence of the region of immobilization has been suggested only in cases of cations with a small radius (Li^+, Na^+), anion F^-, or ions with 2+ charges. In the present calculation, the partial charge for each charged group is smaller than unity. The region of immobilization observed in our simulation of melittin in water may be caused by the existence of multiple partial charges close in space. The evidence for structure breaking will be further supported later by the analysis of the life times of the water–water H-bonds of the C1 and C2 water molecules. In both the first and second shells, the N1 and N2 water molecules have the longest τ_1 and τ_2 values. This result may be related to the difference of the water–water H-bond network between the N1 class and other first-shell classes. This will be discussed in the following section.

D. Water–Water and Protein–Water Hydrogen Bonds. Histograms of the number of the water–water H-bonds and the lifetimes of the H-bonds are shown in Figure 6 and Table IV, respectively. Lifetimes of protein–water H-bonds are also shown in Table V. As seen in Table IV, the lifetimes of water–water H-bonds in C1 and C2 classes are apparently shorter than others. These short lifetimes correspond to what we described as structure breaking and are caused by the presence of a chloride ion and/or a charged group. The short lifetime of H-bond in C1 and C2 classes is caused by the difference of mobilities of the C2 class from others. The lifetimes of P1 and N1 classes are almost the same as that of the pure class. In the second shell the lifetimes are shorter than that of bulk. We can also observe differences

TABLE IV: Life time of the Water-Water Hydrogen Bond

class	life time I[a] psec	life time II,[b] psec	no. of H-bonds[a]
C1 (charged1)	1.0	1.5	2.4
P1 (polar1)	1.3	2.0	2.9
N1 (nonpolar1)	1.3	2.0	3.3
C2 (charged2)	0.9	1.5	3.5
P2 (polar2)	1.2	1.7	3.6
N2 (nonpolar2)	1.2	1.8	3.6
bulk	1.4	2.0	3.7
pure	1.3	1.9	3.7

[a] Calculated by using definition I. [b] Definition II. Definition of the life time is given in the text.

TABLE V: Life time of the Protein-Water Hydrogen Bond

type	life time I,[a] psec	life time II,[b] psec	av no. of H-bonds[a,c]	average number of H-bonds[a,d]
charged	1.4	2.0	1.1	4.6
polar	0.8	1.7	1.0	1.2

[a] Calculated by using definition I. [b] Definition II. Definition of the life time is given in the text. [c] Per each water molecule. [d] Per each group.

in the number of H-bonds. The shapes of the histograms are also very similar to each other except for that of the first shell. More than 50% of water molecules in the second shell as well as bulk and pure classes have four H-bonds. Peak positions in C1 and P1 are all at three H-bonds. In the case of C1, the height of the peak at two H-bonds is almost the same as that for three bonds. As shown in Table IV, the average number of water–water H-bonds in C1 and P1 classes is less by 1.3 and 0.8 than those for bulk and pure classes, respectively. The loss of water–water H-bonds in the C1 and P1 classes is compensated by protein–water H-bonds. In Table V, the number of protein–water H-bonds per water molecule in charged and polar types is 1.1 and 1.0, respectively. This indicates that the structure of the hydrogen-bond network around charged and polar groups is similar to that of pure water. Generally the number of water–water H-bonds decreases when a water molecule is in contact with a solute molecule due merely to the volume exclusion effect.[21] However, the number of H-bonds in class N1 is less by only 0.4 compared with that in the bulk. This implies that the structure of the hydrogen-bond network around a nonpolar group is different from that of pure water. The results are in accordance with earlier work concerning a small solute, alanine dipeptide.[6] The increase in hydrogen-bond number in class N1 confirms the usual view that the hydrogen-bond network becomes more developed around nonpolar groups. The lifetime of protein–water H-bonds in class C1 is the same as that of water–water H-bonds in the bulk class. On the other hand, the lifetime of the protein–water H-bond in class P1 is much shorter than that of the water–water bond in the bulk class. This result can be ascribed to the difference in the depth of the pair potential energy minima, which is in turn attributed to the magnitude of the partial charges on the groups. We shall discuss this point in the next section.

E. Hydrogen Bond in Each Residue. In Figure 7, the time-averaged total number of protein–water H-bonds, n_{HB}, in each residue is shown. Many bonds are formed near the N-terminus and the C-terminus, while fewer bonds can be seen in the middle of melittin. This is because those groups are free from intramolecular H-bonds. Positions of peaks are at every three to five residues. This is because melittin is an amphipathic molecule consisting of α-helices with hydrophilic residues located mainly on one side of the helices. Numbers of H-bonds for the main chain and for the side chain are also shown in Figure 7. The Lys7, Lys21, and Lys23 side chains from 2.9, 3.6, and 5.2 H-bonds with water molecules, respectively. The 1.6–2.3 difference in H-bond number is caused by the existence of the chloride ion in contact. One chloride ion is in contact with the NH_3 groups of both Lys7 and Lys21 but not in contact with the NH_3 of Lys23. A similar result is also observed in the case of Arg. The Arg22

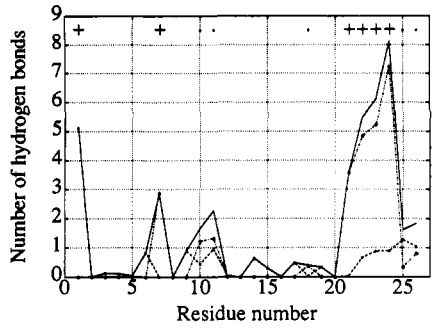

Figure 7. Time-averaged number of protein–water hydrogen bonds in each residue. Numbers in total (—), main chains (- - -), and side chains (· · ·) are shown. The residues indicated by "+" have charged side-chain groups and the residue indicated by "·" have polar side-chain groups.

TABLE VI: Number of Hydrogen Bonds between Water and Protein in Each Energy Criterion Is Shown

	no. of H-bonds main/side		
residue	−3.0 kcal/mol	−2.0 kcal/mol	−1.0 kcal/mol
N-terminus	5.1	5.8	6.1
Arg	0.8/6.0	1.1/6.6	1.4/7.0
Lys	0.3/3.9	0.5/4.1	0.7/4.2
Thr	0.7/1.3	1.0/1.4	1.2/1.7
Gln	1.2/0.6	1.7/1.2	2.2/2.7
Ser	0.0/0.4	0.1/0.5	0.2/0.7

side chain with two chloride ions in contact forms 3.6 H-bonds, while the Arg24, which has no chloride ions in contact, forms 7.2 H-bonds. From these results, we can conclude that one chloride ion replaces more than one water molecule in contact and reduces the number of H-bonds by about 1.5–2.

In order to examine the differences in the number of H-bonds among residues, we change the energy criterion from −3.0 kcal/mol to −2.0 and −1.0 kcal/mol. The results are shown in Table VI. When the energy criterion is changed, only small differences are observed in the number of H-bond of the Lys side chains (only 0.3 difference between −3.0 and −1.0 kcal/mol criteria). In other words, the number of H-bond is less sensitive to the criteria for those residues. It is because their partial charges are large compared with others and the minima of the pair potential energies are deep and broad. However, in the Gln side chains, differences are rather large (2.1 difference). This is because the interactions between water molecules and these side chains are weak.

F. Correlation between Conformational Transition and Change in Hydration Structure. We reported in the previous paper[3] that a conformational transition of melittin takes place along the first few principal axes, which are calculated from the MD trajectories. The first principal axis is defined such that atomic fluctuations have the largest value in this axis. The second principal axis is orthogonal to the first one and is defined such that atomic fluctuations have the second largest value in this axis. These principal axes correspond very closely to the lowest few normal mode axes of melittin in vacuum. In the previous paper, we compared breakdowns of the average potential energy over the first 20 ps (before transition) with those over the last 20 ps (after transition). Large differences were seen in the energy between protein and water molecules (17.9 kcal/mol increase) and among water molecules (15.4 kcal/mol decrease). Here we will show that these energy changes are related to the change of hydration structure.

First we examine the number of first-shell water molecules and the number of H-bonds, n_{HB}. In Figure 8, we show the time evolution of these values. Projections of MD trajectories onto the first and the second principal axes are also shown. The beginning (at about 23 ps) and the end (at about 29 ps) of the transition are shown by the vertical dotted lines. After the transition, the conformation of melittin becomes straighter and the hydrophobic side is more exposed. Associated with this

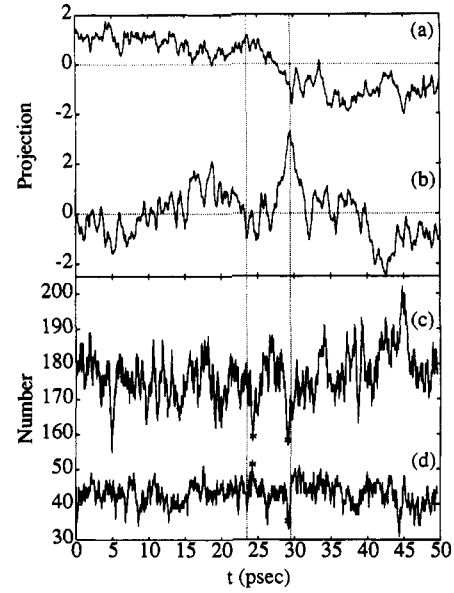

Figure 8. Time evolutions of the projections of the MD trajectories onto (a) the first and (b) the second principal axes, (c) total number of first-shell water molecules, and (d) total number of protein–water hydrogen bonds. The vertical lines (· · ·) indicate the beginning and the end of conformational transition. The meaning of the "*" is explained in the text. (a) and (b) are scaled by each standard deviation along the axis (0.16 Å (a), 0.13 Å (b)).

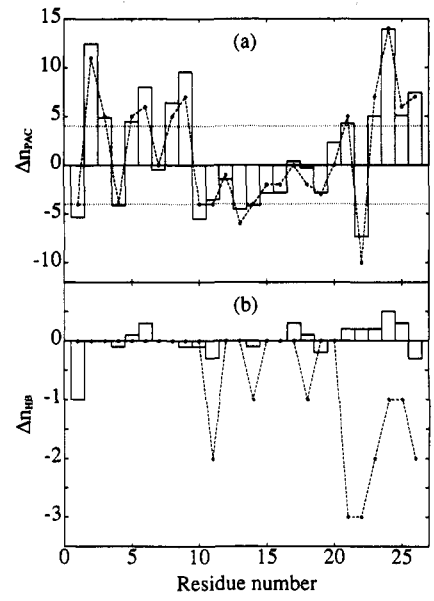

Figure 9. (a) Differences of n_{PAC} per residue between the first 20-ps average and the last 20-ps average and those between two V-structures indicated by "*" in Figure 8. They are shown by the histogram and (- - -), respectively. (b) Equivalent for n_{HB}.

transition, an appreciable change in the number of first-shell water molecules and n_{HB} may be expected. However, the average numbers of first-shell water molecules and n_{HB} over the last 20 ps are greater by only 3.9 and 0.07 than those over the first 20 ps, respectively. To pursue further the possible correlation between the conformational transition and hydration structure change, we examine the local hydrogen-bond network and packing topology. Instead of examining the number of first-shell water molecules, we examine the number of atom pairs, n_{PAC}, between protein atoms and water oxygen atoms that are in contact. When n_{PAC} is averaged over a sufficient time interval, it gives the running coordination number at the distance $k\sigma_{ij}$. We examine the differences of n_{PAC} and n_{HB} per residue between the first 20-ps average and the last 20-ps average, Δn_{PAC} and Δn_{HB}. They are shown in Figure 9a. The total n_{PAC} increases by 38.7 after the

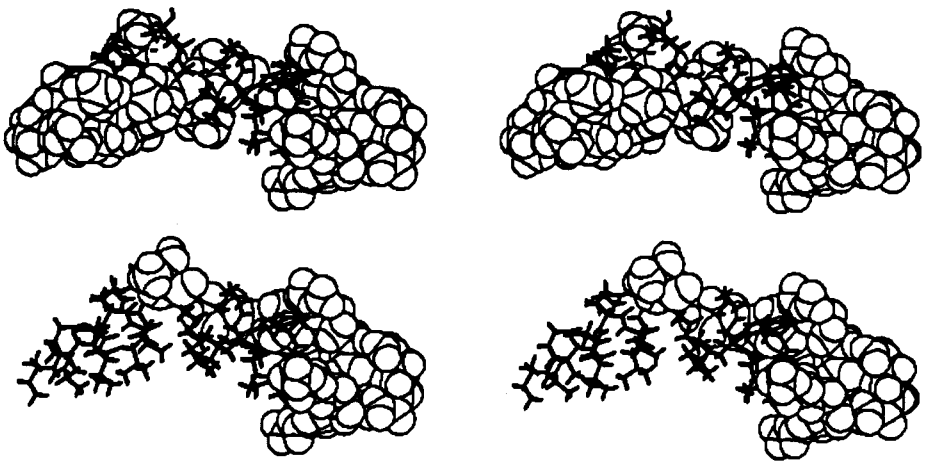

Figure 10. (a, Top) Residues with large changes in n_{PAC} are shown for the CPK model. (b, Bottom) Residues where n_{HB} changed between the two V-structures indicated by "*"s in Figure 9 are shown for the CPK model.

transition. There is a clear tendency for the Δn_{PAC}'s to be positive in the residues near the N-terminus and the C-terminus and negative in the middle of the two regions. In Figure 8 of the reference,[3] the root-mean-square fluctuation of each C^{α} atom is shown. Two nodes are seen at about the 10th and 20th residues. The outer two regions move in the same phase and the middle region moves in the opposite phase. Clear correspondence can be seen in the Δn_{PAC}. A further feature is that negative peaks appear every third residue (Gly1, Ala4, Lys7, Thr10, Leu13, Trp19, and Arg22 except for Leu16 and Gln25). These residues are located on one side of melittin, which is one of the two sides between the hydrophobic and the hydrophilic sides. These two results suggest that there is a close correlation between the direction of the conformational transition and the change in the intermolecular packing topology.

The residues for which the n_{PAC}'s change by more than 4.0 are shown in Figure 10a. These residues form two groups, one near the N-terminus and the other near the C-terminus. As shown in Figure 8a,b, the transition occurs mainly in the space corresponding to the first and second principal axes. When melittin moves along these two principal axes, atoms in these two regions deviate significantly from the average position. This indicates that change of hydration structure of solvent water molecules is closely correlated with the collective motions of the protein incurring the conformational transition.

The changes of n_{HB}, Δn_{HB}, are shown in Figure 9b. The magnitude is small (less than or equal to one H-bond). This may be because in both of the two states the hydrogen bonds between the protein and water are maximized. Thus, in the particular transition we discussed, packing topology rather than hydrogen bonding played a major role.

These results are consistent with the analysis by ASA as follows: The change of average ASA in nonpolar groups is 68 Å^2. However, the change in charged and polar groups is only 4 Å^2. This confirms the conclusion that hydrogen bonding did not play a major role in the transition.

In addition to the comparison of the average values, we also check the change in n_{PAC} and n_{HB} at the beginning and at the end of the transition marked by "*"s in Figure 8. They are also shown in Figure 9. It should be noted that the behavior of the dashed line and the histogram is very similar in Figure 9a. The residues whose H-bond numbers change between the two "*"s are shown in Figure 10b. In this case large changes in n_{HB} as well as in n_{PAC} are observed. From these results we conclude that the two averaged states before and after the transition differ mainly in the atom packing between protein and water molecules shown in Figure 10a, but the difference in H-bond number is small due to the reason previously mentioned. During a transition period between the averaged two states, both packing topology and hydrogen-bond network are significantly changed.

IV. Conclusion

In this paper, we carried out a molecular dynamics simulations of protein and water and of pure water. Trajectories of coordinates and velocities were collected for 50 ps. From the trajectories, we calculated the V-structure of water, ion, and melittin. We analyzed the changes in packing topology and hydrogen-bond network and also analyzed the characteristics of translational and rotational motions. We found that the lifetimes of water–water H-bonds around charged groups and ions are shorter than those of other water–water H-bonds. The lifetime of H-bonds between water and charged groups of the protein is close to that between a water pair. However, the bonds between water and polar group are weaker and their lifetime is shorter than that of bulk water. Translational and rotational motions of water around protein are slower by 40–50% than those of pure water. Mobilities of water molecules are restrained by interaction with protein.

We also observe a correlation between protein motions and the changes in intermolecular atom packing and H-bonds. We find a clear correlation between the change in atom packing and the conformational transition, observed in the previous paper. The difference of atom packing between the fist 20 ps and the last 20 ps is mainly seen in the residues with coordinates that deviate substantially from their average positions during the conformational transition. However, the change in the number of H-bonds is less than unity. In the middle of the transition, large changes are observed both in atom packing and H-bonds. From these results we conclude that the conformational transition observed in the previous article is caused by the changes in packing topology that take place during the collective motions of melittin. In support of this conclusion, we have carried out a free energy analysis of melittin in water based on the extended RISM theory.[22] The results will be presented in the following paper.[23]

Acknowledgment. We express our thanks to Dr. Hayward for reading the manuscript carefully. Computations were done at the Computer Centers of Kyoto University and of the Institute for Molecular Science. This work has been supported by grants from the Ministry of Education, Science and Culture, Japan, and from the International Human Frontier Science Program Organization.

References and Notes

(1) (a) Van Gunsteren, W. F.; Berendsen, H. J. C.; Hermans, J.; Hol, W. G. J.; Postma, J. P. M. *Proc. Natl. Acad. Sci. U.S.A.* **1983**, *80*, 4315. (b) Levitt, M.; Sharon, R. *Proc. Natl. Acad. Sci. U.S.A.* **1988**, *85*, 7557. (c) Brooks, C. L., III; Karplus, M. *J. Mol. Biol.* **1989**, *208*, 159.

(2) Jorgensen, W. L.; Tirado-Rives, J. *Chem. Scr.* **1989**, *29A*, 191.
(3) Kitao, A.; Hirata, F.; Gō, N. *Chem. Phys.* **1991**, *158*, 447.
(4) Geiger, A.; Rahman, A.; Stillinger, F. H. *J. Chem. Phys.* **1979**, *70*, 263.
(5) Mezei, M.; Beveridge, D. L. *J. Chem. Phys.* **1981**, *74*, 6902. Karim, O. A.; McCammon, J. A. *J. Am. Chem. Soc.* **1986**, *108*, 1762.
(6) Rossky, P. J.; Karplus, M. *J. Am. Chem. Soc.* **1979**, *101*, 1913.
(7) Eisenberg, D.; Kauzmann, W. *The Structure and Properties of Water*; Oxford University Press: New York, 1969.
(8) Hirata, F.; Rossky, P. J. *J. Chem. Phys.* **1981**, *74*, 6867.
(9) Postore, A.; Harvey, T. S.; Dempsey, C. E.; Campbell, I. D. *Biophys. J.* **1989**, *16*, 363.
(10) Kitchen, D. B.; Hirata, F.; Kofke, D. A.; Westbrook, J. D.; Levy, R. M.; Kofke, D.; Yarmush, M. *J. Comput. Chem.* **1990**, *11*, 1169.
(11) Berendsen, H. J. C.; Postma, J. P. M.; van Gunsteren, W. F.; Hermans, J. In *Intermolecular Forces*; Pullman, B., Ed.; Reidel: Dordrecht, Holland, 1981; p 331.
(12) Andersen, H. C. *J. Comput. Phys.* **1983**, *52*, 24.
(13) Berendsen, H. J. C.; Postma, J. P. M.; van Gunsteren, W. F.; DiNola, A.; Haak, J. R. *J. Chem. Phys.* **1984**, *81*, 3684.
(14) Tanaka, H.; Ohmine, I. *J. Chem. Phys.* **1987**, *87*, 6128.
(15) Evans, D. J.; Murad, S. *Mol. Phys.* **1977**, *34*, 327.
(16) Eckart, C. *Phys. Rev.* **1935**, *47*, 552.
(17) Noguti, T.; Gō, N. *Proteins*, **1989**, *5*, 97. Noguti, T.; Gō, N. *Proteins* **1989**, *5*, 104. Noguti, T.; Gō, N. *Proteins* **1989**, *5*, 113. Noguti, T.; Gō, N. *Proteins* **1989**, *5*, 125. Noguti, T.; Gō, N. *Proteins* **1989**, *5*, 132.
(18) Ishimura, M.; Uedaira, H. *Bull. Chem. Soc. Jpn.* **1990**, *63*, 1.
(19) Frank, H. S.; Wen, W.-Y. *Discuss. Faraday Soc.* **1957**, *24*, 133.
(20) Samoilov, O. Y. *Discuss. Faraday Soc.* **1957**, *24*, 141. Geiger, A. *Ber. Bunsenges. Phys. Chem.* **1981**, *85*, 52.
(21) Hirata, F.; Rossky, P. J. *J. Chem. Phys.* **1981**, *74*, 5324.
(22) Hirata, F.; Rossky, P. J.; Pettitt, B. M. *J. Chem. Phys.* **1983**, *78*, 4133.
(23) Kitao, A.; Hirata, F.; Gō, N., *J. Phys. Chem.*, following paper in this issue.